THERMAL CONTROL FOR ELECTRIC VEHICLE BASED ON THE MULTI-STACK FUEL CELL

Mohammed Amine Chetouane [1 2], Belkhir Negrou [1], Mohamed Becherif [3], Noureddine Settou[1], Abdessalem Bouferrouk[4], Mohamad Ramadan [5]*

[1] *Lab. Promotion et valorisation des ressources sahariennes (VPRS), University of Kasdi Merbah Ouargla, BP 511, Route de Ghardaïa, Ouargla, 30000, Algeria*

(not needed as it's the same university)

[3] *FEMTO-ST Institute, FCLAB, Univ. Bourgogne Franche-Comté, CNRS, Belfort, France.*

[4] *Department of Engineering Design and Mathematics, University of the West of England, Bristol BS16 1QY, UK*

[5] *Energy and Thermo-Fluid Group, School of Engineering, The International University of Beirut (BIU), Beirut, Lebanon.*

[*]Corresponding author: chatmohamin@gmail.com

Abstract. Pollution, global climate change, and the scarcity of fossil fuel reserves have forced the automotive industry to step up its research efforts on clean fuel cell electric vehicles (FCEVs). In fact, these systems can be considered relatively pollution-free systems, with zero greenhouse gas emissions and higher efficiency than traditional vehicles. FCEVs typically use two sources of energy, fuel cells (FCs) and supercapacitors (SCs). One of the main issues with FCs is keeping the temperature between 60 and 90 °C. In this paper, a strategy for controlling the temperature of the FC is proposed. Its objective is to achieve two main goals: the first is reducing the time and energy required to reach the optimum temperature, and the second is maintaining the temperature of the FC in the ideal range during operation. A SIMULINK / MATLAB model has been established to determine the efficiency of the proposed system. The results show that at low ambient temperatures, the FC can be heated within 6 minutes, moreover the system allows cooling the FC and keeping its temperature in the ideal range.

Keywords: electric vehicles, thermal management, fuel cell, multi-stack, heating and cooling

1. INTRODUCTION

The exploitation and widespread use of non-renewable, fuel-based energy sources as a result of improved living standards and economic development has led to serious problems such as energy crisis and pollution of the environment. Within this context, 40% of fuel consumption is related to transport sector [1] and according to [2] the greenhouse gas emissions accounted for a quarter of total emissions in 2016. That is why, many fuel cell electric vehicles (FCEVs) models are being developed by different manufacturers such as Toyota Mirai, Hyundai ix35 fuel cell, and Mercedes GLC F-Cell. Such systems offer many benefits: energy savings, being pollution-free, high efficiency, and low noise. Using the fuel cell (FC) as the main source and the energy storage system (ESS) as an auxiliary source allows combining the advantages of each type of energy source. Usually, there are three different combinations that are possible including FC - Battery, FC - SC, and FC - SC – Battery [1,3,4]. This family of vehicles replaces fossil fuels by hydrogen because it is not a polluting element, and the specific energy of hydrogen is $120\ MJ/kg$, while that diesel and gasoline is approximately $46\ MJ/kg$ [5,6]. That said, hydrogen does not exist naturally and thus it should be obtained from primary elements such as water, biomass, natural gas, coal, and other sources. [7–15]. The Proton Exchange Membrane (PEM) fuel cell is a device that transforms chemical energy into electrical energy thanks to a chemical reaction between hydrogen and oxygen and the byproducts are water and heat energy. The operating temperature should be between $60\ °C$ and $90\ °C$, supplying power between $100\ W$ and $500\ kW$ with an efficiency of 60%, the solid polymer membrane is resistant to vibrations, and the life span of the FCs is 500 – 1000 cycles [3,16–18]. The supercapacitor (SC) is an electrical component consisting of two parallel conducting plates separated by a dielectric medium with specific energy of $(1-10)\ Wh/kg$, specific power of $10000\ W/kg$, efficiency $(85-98)$ %, and cycle-life of more than 500000 [19]. The battery is a device that stores energy in the form of electrical energy by taking advantage of the electrochemical process reversibility to recover it, with specific energy of $(100 - 200)\ Wh/kg$, specific power of $(1000\ to\ 3000) W/kg$, and cycle-life more than 500 [20].

In recent years, a lot of research has been done on FC / ESS, e.g. in [21] the authors presented a comparison between 575 articles published between 1998 and 2014 on the field of energy management for hybrid electric vehicles. In [22], the authors reviewed challenges in integrating and optimizing renewable hybrid energy systems, with a focus on those using hydrogen energy. In [23], the authors focused on the different constraints generated and their impacts on the different components of the FC. In [24] , the authors studied a new engine group concept, with a dual-energy system, on a fuel cell in order to reduce fuel consumption with different energy management strategies that were studied, where the authors applied different tests, including the authenticity of genetic algorithms that minimize energy consumption. In [25], a DC bus voltage management and control algorithm based on linear mode controls for the system management was developed to control a hybrid FC / SC system. The proposed energy management model enabled the operating system with three modes depending on the load profile and the state of charge. In [26] the authors dealt with the problem of energy optimization of a hybrid energy storage system composed of a fuel cell (as the main source) and a super capacitor (as an auxiliary source). The study consisted of two different parts: the control stage and the power management system. Researchers in [27] developed a combination between the optimized genetic thermostat strategy under specific driving conditions and the condition recognition method, which could be automatically switched to the optimal energy management strategy under corresponding conditions.In [28] the authors designed the fuel cell vehicle structure, and proposed a new procedure to improve the dynamic performance of the vehicle while meeting the requirements of the vehicle and extending its life time. In [29], the authors used an online computer-controlled transducer to simulate a realistic FC response. In [30] the authors proposed a framework for energy management between a fuel cell and a super-capacitor and compared this strategy with three other methods of energy management; the suggested strategy is based on State of Charge analysis with SOC ≥ 60% and using MATLAB / Simulink. In [31], the authors carried out a modeling study of a fuel cell/battery system, and they proposed an energy management strategy according to the power demand and state of charge, and used the MATLAB / Simulink to study the effect of the initial SOC. Badji et al. [18] proposed a control strategy based on power frequency division for a system with battery and SC as auxiliary devices linked to FC. In [32], the authors proposed a hybrid propulsion system for use in a lightweight aircraft, where they conducted some analyses containing on the required energy, hydrogen consumption, energy consumption, etc.

Temperature, humidification, hydrogen and air supply, as well as many other elements play a critical role in the efficiency, the life, and the safety of PEMFC. The authors in [33] conducted an objective analysis to find the input factors that significantly affect the response variables, relying on the use of Mathematical Model for Simulation Model and MATLAB Simulink. In [34], a study using an experimental database on a Ballard FC used 9 -SSL 21 kW stack to reduce thermal stress and to support the need for a control-oriented model of the PEM fuel cell system to study temperature. The authors proposed in [35] an adaptive control strategy for regulating the fuel cell temperature at the optimum point . In [36], Becherif et al. proposed a multi-stack system installed in parallel with a battery, the idea was to use an adequate number of equivalent fuel cells to meet the required power. The authors in [37] conducted a pilot study of the bubble moisturizer used to moisturize PEMFC. The study included the effect of the water temperature in the tank, the water level inside the tank, and the incoming airflow on the performance of the humidifier. In another study [38], an analysis was performed by numerical simulation of the operating characteristics of the ejectors in the PEMFC system - the ejectors used to recycle hydrogen anode in the PEMFC systems and the study included the effects of four parameters on the performance. In the paper [39], the authors proposed the control on the hydrogen and oxygen flow pressure by Proportional-Integral, fuzzy logic, and artificial neural network-based schemes and the system performance was tested under different operating conditions for each controller, again assisted by MATLAB /Simulink. The authors in [40] conducted experiments to investigate the phenomenon of local degradation in PEMFCs during dead-ended anode processes.

Heat management is one of the research hotspots in the development of FCEV. In order to achieve optimum operation, the FC must be heated up before starting because the FC is at a low temperature before operation, then after the FC starts, , it loses a large amount of energy as heat. For this reason, it must be cooled to keep it at an appropriate temperature.

In this work, a fuel cell heat management strategy is proposed for vehicles. The study mainly includes two processes: the first is the process of heating the FC so that it can be used in ideal conditions with high efficiency and low hydrogen consumption. The FC is split into two categories to minimize dependence on previously stored energy in the ESS and, as a result, the size of the storage element. The cooling of the multi-pack FC system is the second process, which aims to maintain the temperature stability of the fuel cell within an ideal temperature range.

In order to study the efficiency of the proposed system, a simulation model was prepared within the framework of the MATLAB program and used in order to subject the system to the necessary experiments to evaluate its efficiency.

2. System Description

Generally, the energy source system in FCEV is composed of one FC and the ESS. However, the decomposition of the FC stack to a multi-pack system has several advantages, such as facilitating maintenance work, FCs can be replaced separately because they are installed in parallel, and it can also take advantage of the aspect of controlling the number of FCs turned on depending on the average power demand while driving. As for this work, the benefit of the multi-pack FC is the ability to heat only a small FC by relying on ESS, and then take advantage of that small FC that was heated to provide the necessary energy in order to raise the temperature of the other FC pack. In theory, this reduces the energy that the ESS would have to provide compared to the case if the FC was heated in normal volume directly, as that reduces automatically the size of ESS.

The multi-pack FC system used in this study (shown in **Figure 1** and **Figure 2**) is composed of two FCs in a parallel connection in the electric system, and in series connection in the cooling system. Each FC in the system has a different number of cells, the first has 20 cells and the

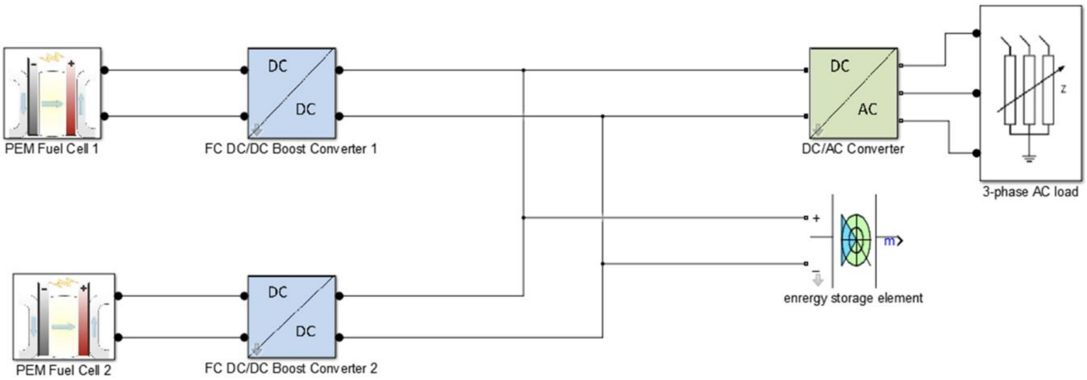

Figure 1: FCs/SC system connection.

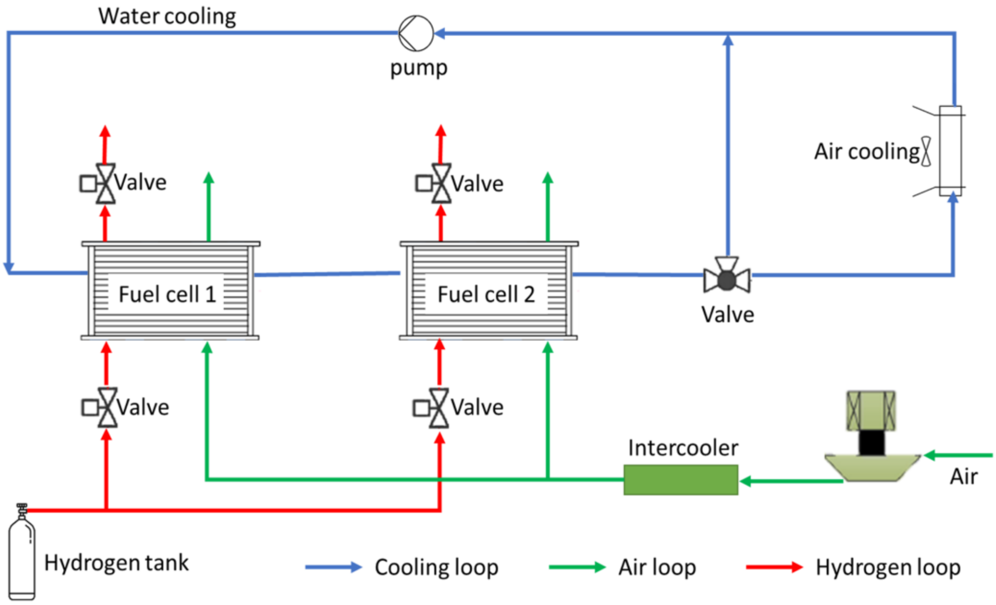

Figure 2: Schematic of cooling system for multi-pack fuel cell.

second has 110 cells. The active area of each FCs is $285.5\ cm^2$. This configuration can, in the maximum operation conduction, generate $33675\ W$ (more characteristics of the fuel cells utilized in the multi-pack FC system are displayed in **Table 2**), and that is enough to request the demand of energy for FCEV run at $130\ km/h$ [35].

The ESS is an important element to ensure that the FCEV is fully supplied with its energy needs without interruption. As for this work, this is even more important as the ESS will also be used to obtain the necessary energy for the primary heating of the FC, for this an ESS is added to system (shewed in Figure 1). Batteries or SC can be used in parallel with a FC to meet the high peaks in demand and can be recharged when the demand is lower by the FC itself. But in **Figure 2** the ESS is not shown because the study did not take into account the effects of temperature on the ESS, and the focus is only on the FC.

The study presented in this paper consists of two cases, the first case is the preheating process and the second case is the cooling process, and within the first case there are two parts, the first is the preheating of the first FC and the second is the preheating of the second FC.

In the case of the heating process, and depending on the FC temperature, and before starting the FCEV, the multi-stack FC was heated to $335K$. During this period, the process is divided into two parts: First, the process uses the energy stored in the ESS to heat the first FC to $335\ K$. At this point, the ESS only supplies the energy necessary for the process. The objective of the first part has been achieved and the process of the second part has been started. In this part, the first FC starts and begins to generate energy. This energy is used to heat the second FC. In this part, the ESS will not contribute. For any energy, only the first FC produces the required power. In this part, the cooling water plays the role of an energy transfer fluid, since it uses the energy absorbed during cooling the first FC to heat up the second FC. This makes the second fuel cell heating process faster and consumes less energy, and when the temperature of the second FC is

335 K, the heating process ends, and then the vehicle can start-up, and also the cooling process can start.

In theory, the fuel cell loses 40 % of the hydrogen energy in the form of heat energy, and in order to keep the operating temperature of the stack within the required range, a portion of this heat must be removed from the stack, by conduction and convection and by cooling the system. In practice, the small FC can be cooled by air, but this is not effective in the FC stacks larger than 10 kW such as the ones used in this study. In the current work, the water is used for cooling the multi-pack FC system and controlling its temperature; this operation is presented in Figure 2 where the coolant water is circulated through the multi-pack FC by a pump, the cooling water absorbs the heat energy from the different FCs and transfers it to the cold airflow stream by means of a radiator-fan.

3. System thermal model

In this section, the nonlinear model which represents the FC system is developed to facilitate the design study. Generally, the energy produced by a FC can be expressed by two different methods: in the first, the total energy produced by the FC is composed of the electric energy P_{elc} and the thermal energy P_{th} (shown in **Equation 1**); but in the second, the energy produced is the product of the reaction energy H_{rec} and molar flow rate of consumed hydrogen $\dot{m}_{hydrogen}$ (shown in **Equation 2**).

$$P_{tot} = P_{elc} + P_{th} \tag{1}$$

$$P_{tot} = \dot{m}_{hydrogen} * H_{rec} \tag{2}$$

$$\dot{m}_{hydrogen} = \frac{i}{2 * F} * n_{cell} \tag{2-1}$$

where $H_{rec} = 285.5\ \text{kJ}/mol$ is the hydrogen enthalpy of combustion, F is the Faraday constant and its value is $96{,}485\ C/mol$, n_{cell} is the number of cells in the FC, and i is the fuel cell operating current. The electrical power generated by the FC stack P_{elc} was evaluated as:

$$P_{elc} = i * v_{cell} * n_{cell} \tag{3}$$

where v_{cell} is the cell voltage and it is defined in terms of the four terms [41,42] as defined in **Equation 4**: the thermodynamic potential E, the activation losses v_{act}, the ohmic losses v_{ohm}, and the concentration losses v_{conc}.

$$v_{cell} = E - v_{act} - v_{ohm} - v_{conc} \tag{4}$$

In this work, the fuel cell operating voltage v_{cell} is calculated by another equation developed from the experimental data of FCvelocity®-9SSL 21 kW stack as presented in **Table 1**, and the new equation is for v_{cell} becomes:

$$v_{cell}(i) = a\, i^3 + b\, i^2 + c\, i + d \tag{5}$$

where $a, b, c,$ and d are calculated and fixed using curve fitting tool in MATLAB and based on the experimental measurements as presented in **Table 1**:

Table 1:Fuel cell stack operating conditions depending on current [31].

Stack Current [A]	Cell Voltage [V]	Stack Power [W]	$\dot{v}_{coolant}$ [l/s]	Coolant Inlet Temperature [K]	Coolant Outlet Temperature [K]	$Q_{coolant}$ [W]
15	0.857	1414	0.15	333.15	334.15	521.95
30	0. 8250	2722	0.16	333.15	336.15	1722.45
60	0.7880	5200	0.18	333.15	339.15	3789.39
120	0.7420	9794	0.20	333.15	340.15	4863.05
180	0.7150	14157	0.21	333.15	341.15	6113.55
240	0.6830	18031	0.24	333.15	341.15	6724.9
300	0.643	21219	0.26	333.15	343.15	9246.74

$$a = -1.5e^{-8}, b = 8.6e^{-6}, c = 0.002, d = 0.88$$

Based on the works of [31,34], the thermal model is influenced by the stored energy which is expressed in terms of the FC temperature P_{stoc}, latent heat P_{lat}, the energy exchanged between FC and the external environment by natural convection P_{loos}, the energy extracted by the cooling water $P_{cooling}$, and the energy absorbed by a FC in the heating operation $P_{heating}$, as shown in **Equations 6 to 10**:

$$P_{th} = P_{stoc} + P_{lat} + P_{loos} + P_{cooling} - P_{heating} \quad (6)$$

$$P_{stoc} = M_{fc} * Cp_{fc} * \frac{dT_{fc}}{dt} \quad (7)$$

$$P_{lat} = \dot{m}_{H2O\_pro} * H_{lat} \quad (8)$$

$$P_{loos} = K_{fc} * A_{fc} * \left(T_{fc} - T_{atm}\right) \quad (9)$$

$$P_{cooling} = \dot{m}_{H2O\_cooling} * Cp_{H2O} * (1 - e^{c}) * \left(T_{fc} - T_{H2O_{in}}\right) \quad (10)$$

where M_{fc} and Cp_{fc} are the mass and the specific heat of FC respectively, according to [31,43] and based on Ballard Mark V stack, an average value of $8.25\ kJ/kg\ K$ is used for Cp_{fc}, while for M_{fc} 7 kg was used for the first FC and $17\ kg$ for the second FC. A_{fc}, and K_{fc} are respectively the external surface of the FC stack (m^2), and the convective heat transfer coefficient (whose value is about$10\ W/m^2K$).

$\dot{m}_{H2O\_pro}$ and H_{lat} are respectively the water produced by FC after the reaction, and the latent heat coefficient of vaporization for water and. $\dot{m}_{H2O\_cooling}$, Cp_{H2O} and $T_{H2O_{in}}$ are the cooling flow rate, coolant heat capacity, and the temperature of cooling water in the inlet of FC stack, respectively. More details of these parameters including definition of c are found in the Appendix.

By the combination between (1) and (6) the energy balance can be written as follows:

$$M_{fc} * Cp_{fc} * \frac{dT_{fc}}{dt} = P_{tot} + P_{heating} - P_{elc} - P_{lat} - P_{cooling} - P_{loos} \quad (11)$$

In this work, the study consists of two cases, the heating case and the cooling case, and in the heating case there are two parts. For Equation (11), this can be written in three different forms as follows.

The first form is to modulate the heating of FC by the energy supplied by ESS:

$$\frac{dT_{fc}}{dt} = \frac{P_{heating} - P_{loos}}{M_{fc} * Cp_{fc}} \tag{12}$$

The second form is to modulate the heating of FC by the energy produced by another FC:

$$\frac{dT_{fc}}{dt} = \frac{P_{heating} + P_{cooling} - P_{loos}}{M_{fc} * Cp_{fc}} \tag{13}$$

The third form is to modulate the operational mode of FC:

$$\frac{dT_{fc}}{dt} = \frac{P_{tot} - P_{elc} - P_{lat} - P_{cooling} - P_{loos}}{M_{fc} * Cp_{fc}} \tag{14}$$

The thermal energy variation related to the gases heated in FC is estimated from the difference between the thermal energy of the gases entering into the FC, whilst the energy of the gases leaving the FC is neglected in this work due to its low effect on stack cooling.

4. Results and Discussion

The dynamics temperature of multi-pack FC stack is given by the solution to **Equations 12**,**13**, and **14**, and to achieve this a Simulink model is prepared in MATLAB R2014b and used to study system efficiency. In this section, the results obtained are presented. Two parts are included in this work, the first is the heating process and the second is the cooling process.

In **Figure 3**, the results of a comparative study are presented, the first case is the heating of the multi-pack FC system based on the proposed heating method, and the second is the heating of only one FC with power output level equivalent to the multi-pack FC. This process can be presented by the different between the heating of the proposed design in this study and the heating of a standard system; the study uses a heating power of 500W for different outside temperatures.

In **Figure 3-a** the energy supplied by ESS to heat the FC system for the two cases is presented, the results show a difference in the energy consumed in the two cases, especially with regard to the lower outdoor temperatures. At an ambient temperature of $T_{atm} = 318.15\ K$, based on the proposed system, the system requires $8000\ J$ to heat the multi-pack FC, and $24500\ J$ when relying on standard methods. For an ambient temperature of $T_{atm} = 298.15\ K$, based on the proposed system, the system requires $21000\ J$ to heat the multi-pack FC, and $73500\ J$ when relying on standard methods. In addition, for an ambient temperature of $T_{atm} = 278.15\ K$, based on the proposed system, the system requires $32500\ J$ to heat the multi-pack FC, and $150500\ J$ when relying on stander methods. This difference in heat energy is due to the size of the heated FC, and the values shown here represent the level of energy that ESS provides to the system during the heating process. It is important to note that the value of the energy consumed in the heating process of multi-pack FC and the value shown in **Figure 3-a** do not represent all the energy consumed by the heating system, but the energy that the system consumes to heat the first FC only. The source of the remaining energy consumed to finish heating the second FC in the multi-pack FC system is the same as for the first FC, which is the advantage of this work, as it will help to significantly reduce the size of the ESS.

Figure 3-b shows the time required to heat the entire fuel cell system in the two cases. At an ambient temperature of $T_{atm} = 318.15\ K$, based on the proposed system, 46 sec is needed to heat the multi-pack FC, and 49 s when relying on standard methods. For an ambient temperature of $T_{atm} = 298.15\ K$, based on the proposed system, the system requires 137 sec to heat the multi-pack FC, and 147 sec when relying on standard methods. Also for an ambient temperature of $T_{atm} = 278.15\ K$, based on the proposed system, the system requires 375 sec

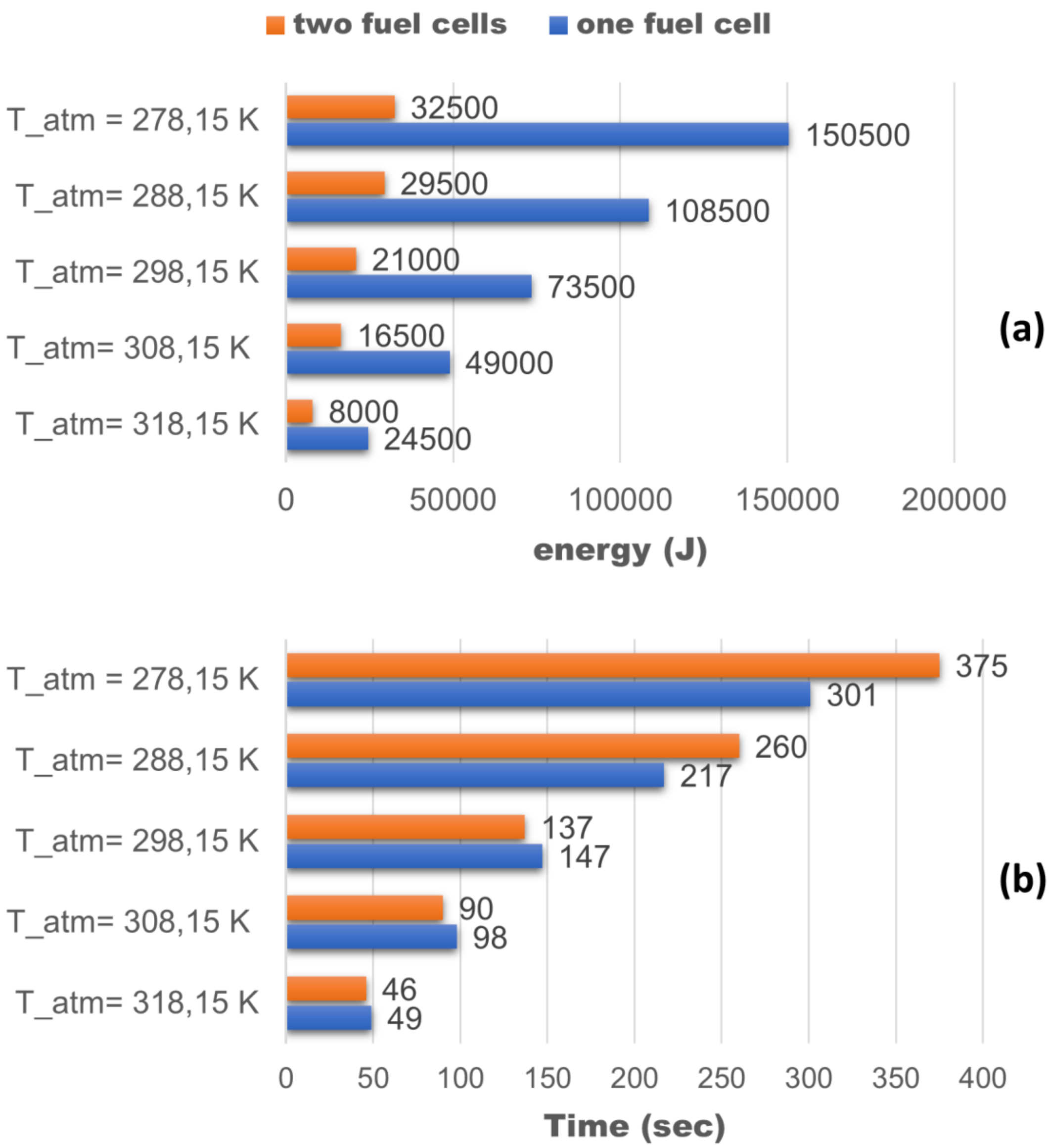

Figure 3a) The energy supplied by ESS to heat the FC system; b) The time required to heat the FCs system.

to heat the multi-pack FC, and 301 sec when relying on standard methods. It can be seen that the time required to heat a fuel cell system at a lower ambient temperature is longer than that required to heat at a higher ambient temperature, and the rate of heating varies with ambient temperature. The results also show that when comparing the heating time of multi-pack FC and standard FC, it varies with ambient temperature. Note that at lower temperatures, standard FCs heat up faster than multi-pack FCs, while multi-pack FCs heat up faster than standard FC configuration when ambient temperature is high, which can be explained by the fact that at lower ambient temperatures the heat exchange with the atmosphere wastes more energy, especially when the exchange area of multi-pack FC is larger than the heat exchange surface of standard FC. This is also due to the fact that, unlike the standard FC configuration, the heating is carried out in two stages.

In **Figure 4** the heating process of multi-pack FC for an ambient temperature of $T_{atm} = 298.15\ K$ using the proposed system is shown. The multi-pack FC heating process takes place in two basic steps: the first step is to heat the first FC in the system using a power of 500 W (shown in **Figure 4-a**) with the process taking about 46 sec. During this period, the FC gets a constant power of 500 watts, and due to heat exchange with the external environment, the FC loses about 300 watts due to the temperature difference. The value of wasted energy is significant because it represents more than half of the energy received by the FC. This may prompt us to recommend adding insulation to the periphery of the FC, but it will weaken the natural cooling of the FC (by natural heat convection) and increase cooling costs. The heating process of the first FC continues until its temperature reaches 335 K, then the process enters the second phase, in which the first FC is working and the energy it generates is used to heat the second FC.

Figure 4-c shows the energy balance undergone by the first FC during the heating process of the second FC. At this point, the first FC is operating and begins to generate the energy

needed to supply the system with the energy needed to heat the second FC and also the power required to start the cooling water pump. At this point, in order to keep the temperature of the FC in the ideal range, the use of the cooling liquid is necessary. Therefore, water is used as a coolant with a constant flow rate of 0.2 l/s, so the energy lost in the process of cooling the first FC is clearly presented with a red color in **Figure 4-c**. The results also show that natural cooling occurs in fuel cells, such as the convection cooling with external media, which is more important than cooling through the water at certain stages. When analyzing the results obtained it can be seen that the energy absorbed by the coolant water decreases with the passage of the heating procedure time, which is due to the increase in the temperature of the coolant water. The increase in coolant temperature is due to the fact that the coolant is not intentionally cooled by the radiator-fan in order to use the energy absorbed by the coolant to heat the second FC.

In the second part, like the first FC, the second FC targets 500 watts of power during the heating process (**Figure 4-d**). As an additional energy source, the second FC benefits from the energy absorbed by the coolant of the first FC, and this reduces the time required to heat up the second FC to $T_{FC} = 335\ K$, which was about 91 sec.

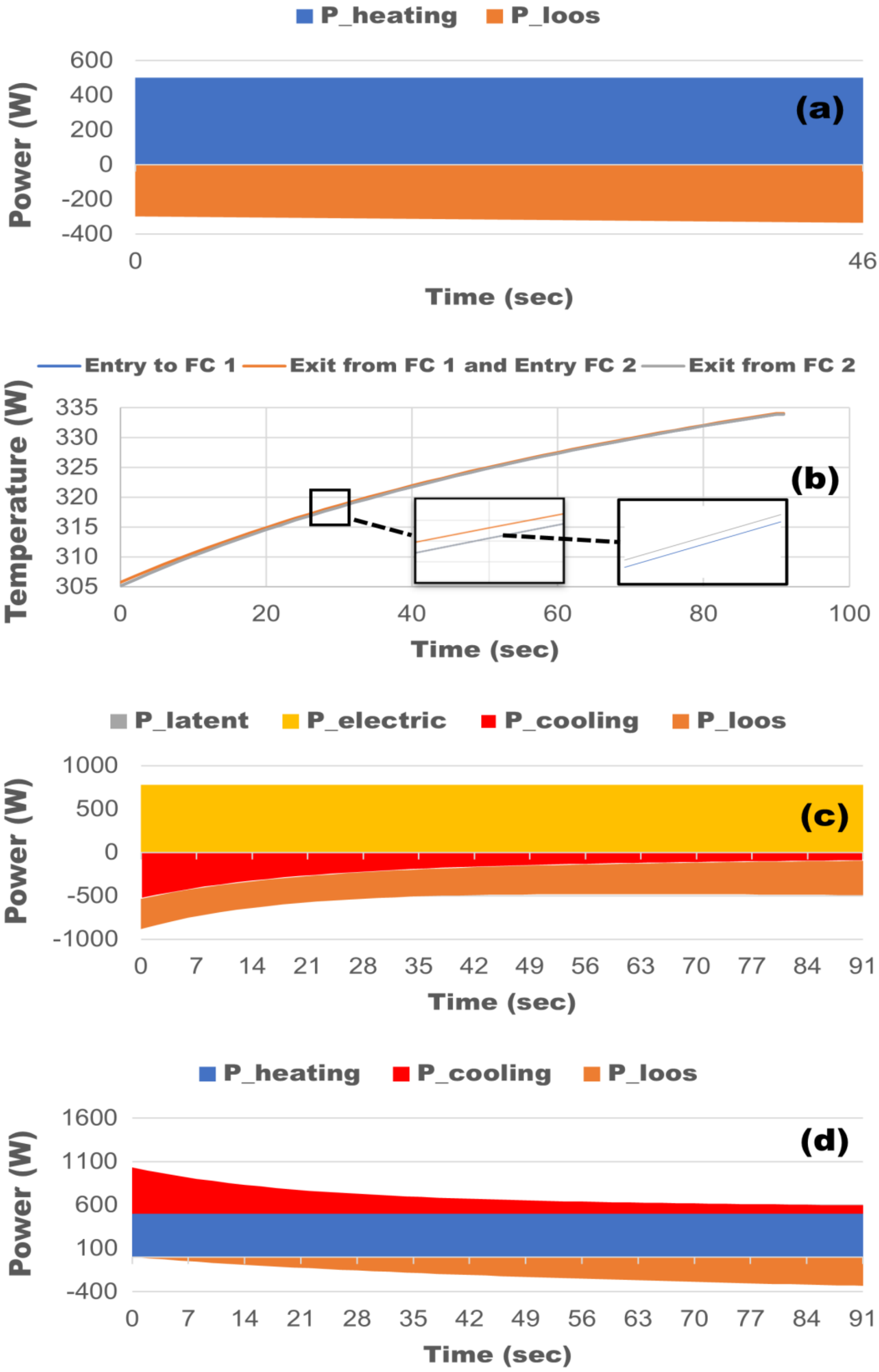

Figure 4: a) The energy balance of the first FC in the first part of the heating; b) cooling water temperature; c) The energy balance of the first FC in the second part of the heating; d) The energy balance of the second FC in the second part of the heating.

The second part of the research is to study the efficiency of cooling systems during operation of multi-pack FC and the ability to maintain the temperature of multi-pack FC within an ideal range, to achieve higher working efficiency. For this reason, multi-pack FC are operated under different electric currents (shown in **Figure 4-a**).

Figure 5-c shows the temperature evolution of the FCs that makes up the system. The results show that at the same current, each FC has a temperature difference with respect to the other FC, in particular, the temperature of the second FC is always higher than the temperature of the first FC, this is mainly due to the size of each FC and the amount of hydrogen consumed during operation. In order to generate the same current, the amount of hydrogen consumed by each FC is different, and essentially the second FC consumes more hydrogen than the first FC. This is due to the number of cells in each FC; the first FC contains 20 cells and the second FC contains 110 cells, therefore, the amount of hydrogen consumed generates more thermal energy, and hence the temperature of the second FC is higher.

In **Figure 5-d**, the temperature changes of the coolant at the outlet of the first FC and at the outlet of the second FC are shown. When the multi-pack FC is in operation, the coolant circulates through the first FC, then through the second FC, at a constant rate of $0.2\ l/sec$. In order to simulate the effect of radiator-fan, the temperature of the coolant at the inlet of the first FC was $333.15\ K$, and at the inlet of the second FC it was considered equal to the temperature of the coolant at the output of the first FC. It can also be observed that the temperature of the heating coolant increases with the increase in the electric current produced by the FC. This is logical when taking into account the results shown in the **Figure 5-d**, where the higher the temperature of the FC, the greater the temperature difference between the coolant and the FC, which means the coolant has absorbed more energy (as shown in **Figure 5-b**), and this results in an increase in the temperature of coolant.

The performance of the proposed model is evaluated in the last part of the study, using ADVISOR (Advanced Vehicle Simulator) software, under the driving conditions to which the vehicle is subjected. ADVISOR is a software that simulates conventional or hybrid vehicles in a standard drive cycle, using the MATLAB environment with the Simulink control for simulation. It was created by the National Renewable Energy Laboratory, or NREL. ADVISOR was distributed for free on the National Renewable Energy Laboratory's website. Between 1998 and 2003, The multi-pack FC was tested on a vehicle weighing 997 kg (**Table 3**), under the EUDC driving cycle, the results are shown in **Figure 6**.

The green in **Figure 6-a** represents the used conduit cycle, while the black signifies the current generated by the multi-pack FC. (The quantity of electric current produced by FC is generally determined by the vehicle's energy demand and the FC contribution to the supply). The results are shown in **Figure 6-b** and **Figure 6-c**, such that the proposed system is able to keep the temperature of the fuel cell in the ideal range for proper operation, confirming the results shown in **Figure 5**.

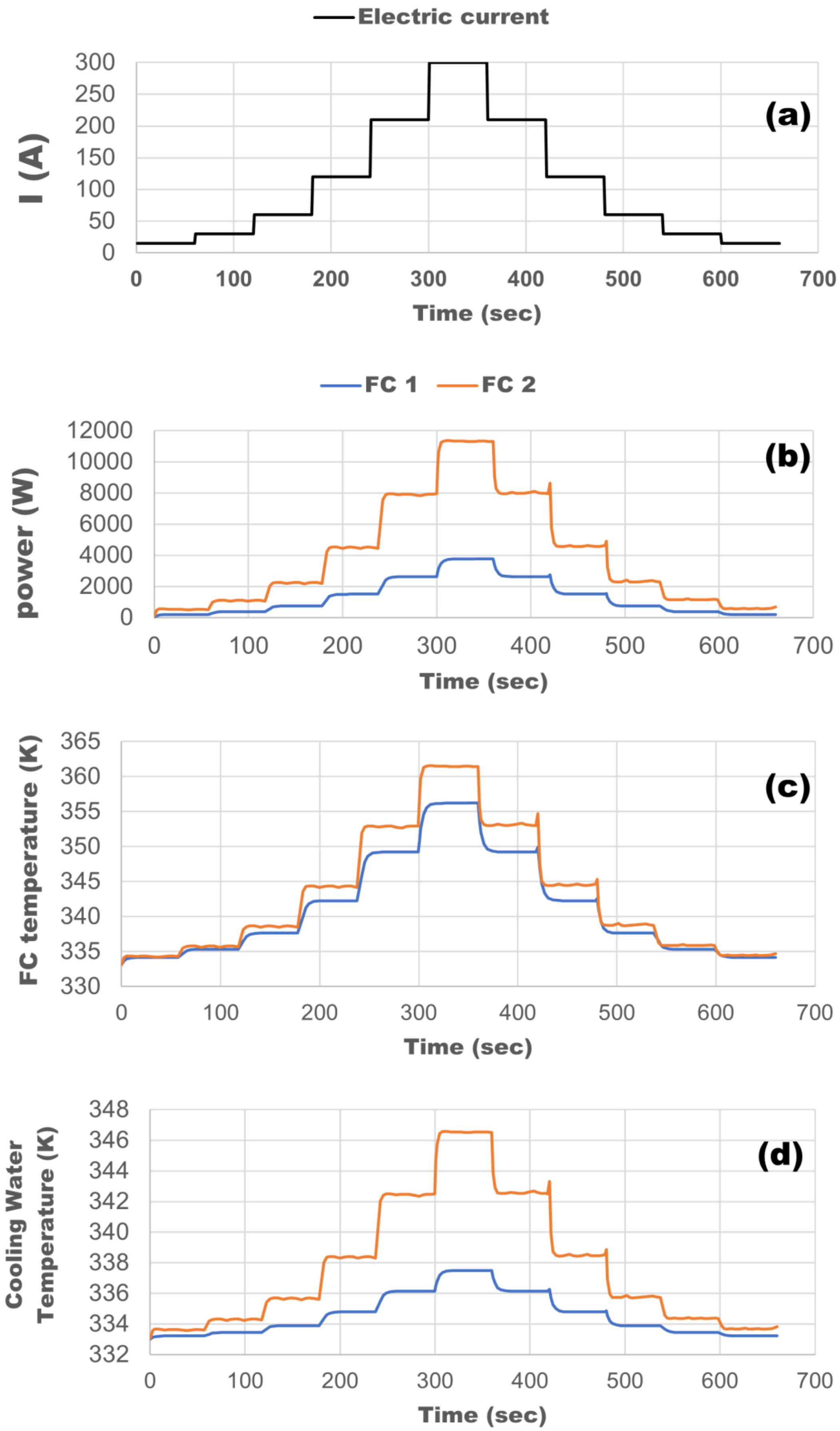

Figure 5: a) Electric current variation; b) cooling power variation; c) multi-pack FC temperature; d) cooling water temperature.

Table 2: Fuel cell parameters.

	Fuel cell 1	Fuel cell 2	Standard Fuel cell
Number of cells	20	110	130
Mass (kg)	6.85	16.75	18.93
Stack core length [mm]	91	306	375
Stack core width [mm]	760	760	760
Stack core height [mm]	60	60	60
Rated Power [kW]	5.3	29	34.2
active area [cm^2]	285.5	285.5	285.5

Table 3 : Vehicle characteristics.

Parameter	Value
Base vehicle mass	997 kg
Gravity acceleration	9.8 m/s^2
Air density	1.2 kg/m^3
Rolling resistance coefficient	0.014
Drag coefficient	0.3
Front area	1.746 m^2
Number of SCs	25
SC mass	0.406 kg
SC specific capacity	7.2 kJ
SC specific power	1.075 kW
Maximum power of FC	34 kW
Power rise rate in FC	2.04 kW
Power drop rate in FC	3.09 kW

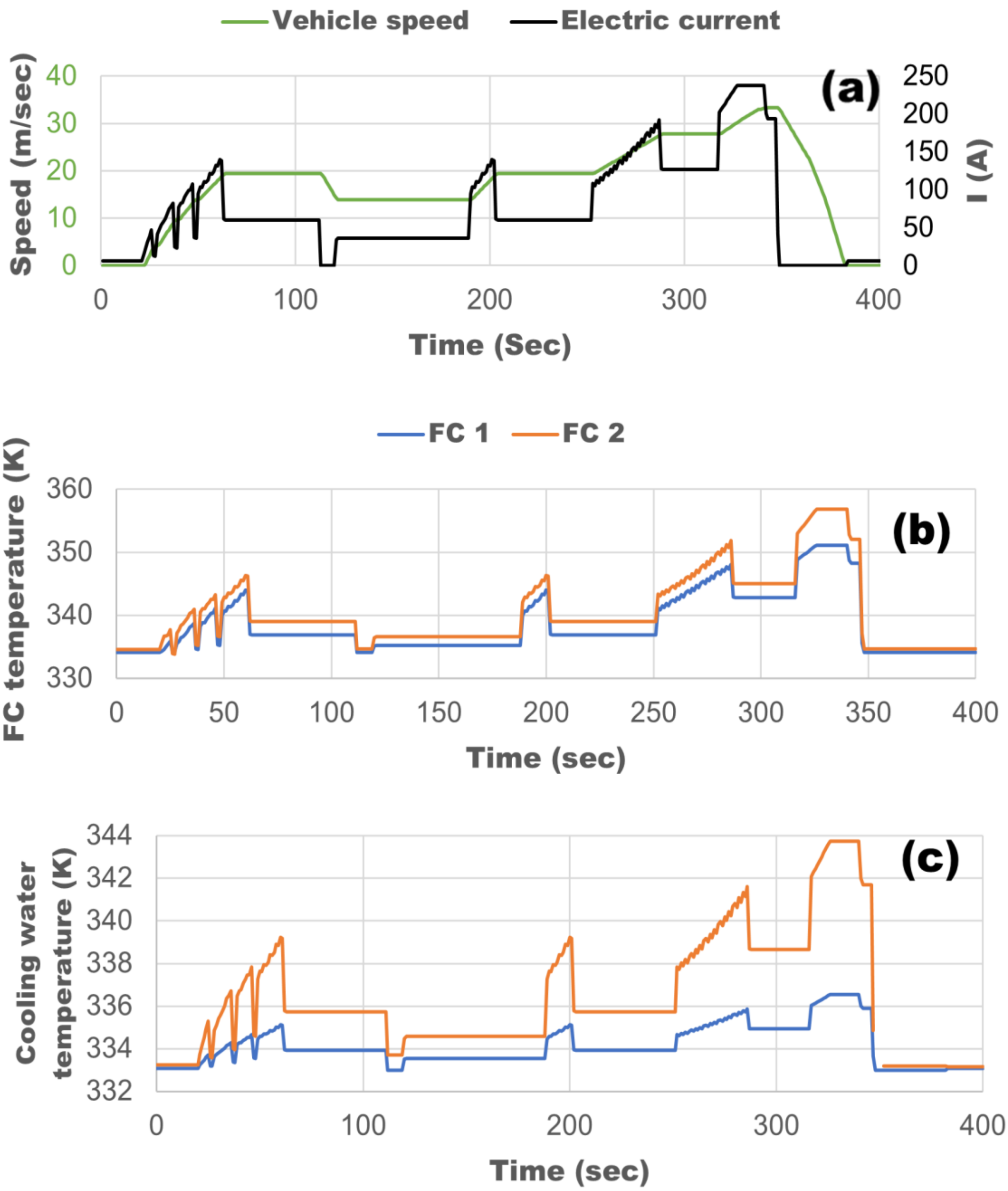

Figure 6:a) Electric current variation; b) multi-pack FC temperature; d) cooling water temperature.

5. Conclusion

Hydrogen is a good alternative to conventional fossil fuels for powering vehicles. For this reason, the development of FC and their use as power sources in stationary applications and vehicles is critical. In this paper, a system has been proposed which aims to heat the FC before operating the vehicle and to maintain the temperature of the FC within a desired range during operation. In some cases, this approach has reduced the energy supplied by the ESS to heat the fuel cell to about a fifth. For an ambient temperature of $T_{atm} = 278.15\ K$, the energy consumed to heat the multi-pack FC is reduced from $150500\ J$ based on standard methods to $32500\ J$ based on the proposed system. The fuel cell heating process, which takes 6 minutes to bring the fuel cell to the desired temperature range and start the vehicle, has also been demonstrated using the proposed system. In addition, the system's performance was investigated when the vehicle was used in cooling operation, and the results showed that the system was efficient in maintaining the fuel cell temperature within the ideal range. The study has found that using a multi-pack FC in the heating and cooling processes is more effective than using a single FC. As a result, future studies would consider how the size gap between the fuel cells that make up the multi-piston system affects the heating and cooling processes, as well as technical and economic aspects.

Acknowledgments

……..

Appendix

H_{lat} in (8) is the latent heat of vaporization of water, which is influenced by the temperature.

$$H_{lat} = 45070 - 41.9\ T_{fc} + 3.44\ e^{-3}\ T_{fc}^2 + 2.54\ e^{-6}\ T_{fc}^3 - 8.98\ e^{-10}\ T_{fc}^4$$

Generally, $P_{cooling}$ calculated as follows:

$$P_{cooling} = \dot{m}_{H2O\_cooling} * Cp_{H2O} * \left(T_{H2O_{out}} - T_{H2O_{in}}\right)$$

where $T_{H2O_{in}}$ is the input temperature of the coolant water, which is measurable and controllable $T_{H2O_{out}}$ is the output temperature of the coolant water, which can be calculated as follow :

$$T_{H2O\_out} = T_{fc} - e^{ln\left(T_{fc} - T_{H2O_{in}}\right) + c}$$

$$c = -\frac{(hA)_{cooling}}{\dot{m}_{H2O_{cooling}} * Cp_{H2O}}$$

Nomenclature

Symbols		Subscript	
FCEV	Fuel cell electric vehicle	atm	atmosphere
ESS	Energy storage system	elc	Electric
P	Power	th	Thermal
F	The Faraday constant	stoc	Stockage
H_{rec}	The reaction enthalpy	lat	Latent
n_{cell}	Cell number	loos	Losing
v_{cell}	Voltage	fc	Fuel cell
i	Electric current	pro	Produce
C_p	The specific heat	tot	Total
M	The mass		
$\dot{m}_{H2O}$	The water flow rate		
H_{lat}	The latent heat of water		
K	The heat transfer coefficient		
A	The surfaces		
T	The temperature		

References

[1] Sulaiman N, Hannan MA, Mohamed A, Majlan EH, Daud WRW. A review on energy management system for fuel cell hybrid electric vehicle: Issues and challenges. Renewable and Sustainable Energy Reviews 2015;52:802–14.

[2] International Energy Agency (IEA). Emissions from fuel combustion highlights 2017:www.iea.org.

[3] Edwards RL, Demuren A. Interface model of PEM fuel cell membrane steady-state behavior. International Journal of Energy and Environmental Engineering 2019;10:85–106. https://doi.org/10.1007/s40095-018-0288-2.

[4] Siangsanoh A, Bahrami M, Kaewmanee W, Gavagsaz-ghoachani R, Phattanasak M, Martin JP, et al. Series hybrid fuel cell/supercapacitor power source. Mathematics and Computers in Simulation 2020.

[5] Barthelemy H, Weber M, Barbier F. Hydrogen storage: recent improvements and industrial perspectives. International Journal of Hydrogen Energy 2017;42:7254–62.

[6] Becherif M, Ramadan HS, Cabaret K, Picard F, Simoncini N, Béthoux O. Hydrogen energy storage: new techno-economic emergence solution analysis. Energy Procedia 2015;74:371–80.

[7] Rahmouni S, Negrou B, Settou N, Dominguez J, Gouareh A. Prospects of hydrogen production potential from renewable resources in Algeria. International Journal of Hydrogen Energy 2017;42:1383–95. https://doi.org/10.1016/j.ijhydene.2016.07.214.

[8] Messaoudi D, Settou N, Negrou B, Settou B, Mokhtara C, Amine CM. Suitable Sites for Wind Hydrogen Production Based on GIS-MCDM Method in Algeria. Advances in Renewable Hydrogen and Other Sustainable Energy Carriers, Springer; n.d., p. 405–12.

[9] Boudries R. Analysis of solar hydrogen production in Algeria: Case of an electrolyzer-concentrating photovoltaic system. International Journal of Hydrogen Energy 2013;38:11507–18. https://doi.org/https://doi.org/10.1016/j.ijhydene.2013.04.136.

[10] Negrou B, Settou N, Chennouf N, Dokkar B. Valuation and development of the solar hydrogen production. International Journal of Hydrogen Energy 2011;36:4110–6.

[11] Chennouf N, Settou N, Negrou B, Bouziane K, Dokkar B. Experimental study of solar hydrogen production performance by water electrolysis in the south of Algeria. Energy Procedia 2012;18:1280–8.

[12] Messaoudi D, Settou N, Negrou B, Settou B. GIS based multi-criteria decision making for solar hydrogen production sites selection in Algeria. International Journal of Hydrogen Energy 2019;44:31808–31.

[13] Settou B, Settou N, Gouareh A, Negrou B, Mokhtara C, Messaoudi D. GIS-Based Method for Future Prospect of Energy Supply in Algerian Road Transport Sector Using Solar Roads Technology. Energy Procedia 2019;162:221–30. https://doi.org/10.1016/j.egypro.2019.04.024.

[14] Messaoudi D, Settou N, Negrou B, Rahmouni S, Settou B, Mayou I. Site selection methodology for the wind-powered hydrogen refueling station based on AHP-GIS in Adrar, Algeria. Energy Procedia 2019;162:67–76.

[15] Rahmouni S, Settou N, Negrou B, Gouareh A. GIS-based method for future prospect of hydrogen demand in the Algerian road transport sector. International Journal of Hydrogen Energy 2016;41:2128–43.

[16] Gong A, Verstraete D. Fuel cell propulsion in small fixed-wing unmanned aerial vehicles: Current status and research needs. International Journal of Hydrogen Energy 2017;42:21311–33. https://doi.org/10.1016/j.ijhydene.2017.06.148.

[17] Dokkar B, Settou NE, Imine O, Saifi N, Negrou B, Nemouchi Z. Simulation of species

transport and water management in PEM fuel cells. International Journal of Hydrogen Energy 2011;36:4220–7.

[18] Badji A, Abdeslam DO, Becherif M, Eltoumi F, Benamrouche N. Analyze and evaluate of energy management system for fuel cell electric vehicle based on frequency splitting. Mathematics and Computers in Simulation 2020;167:65–77.

[19] González A, Goikolea E, Barrena JA, Mysyk R. Review on supercapacitors: technologies and materials. Renewable and Sustainable Energy Reviews 2016;58:1189–206.

[20] Gidwani M, Bhagwani A, Rohra N. Supercapacitors: the near Future of Batteries. International Journal of Engineering Inventions 2014;4:22.

[21] Andari W, Ghozzi S, Allagui H, Mami A. Design, Modeling and Energy Management of a PEM Fuel Cell / Supercapacitor Hybrid Vehicle. IJACSA) International Journal of Advanced Computer Science and Applications 2017;8:273–8.

[22] Eriksson EL V, Gray EM. Optimization and integration of hybrid renewable energy hydrogen fuel cell energy systems–A critical review. Applied Energy 2017;202:348–64.

[23] Dafalla AM, Jiang F. Stresses and their impacts on proton exchange membrane fuel cells: A review. International Journal of Hydrogen Energy 2018;43:2327–48. https://doi.org/10.1016/j.ijhydene.2017.12.033.

[24] Álvarez Fernández R, Corbera Caraballo S, Beltrán Cilleruelo F, Lozano JA. Fuel optimization strategy for hydrogen fuel cell range extender vehicles applying genetic algorithms. Renewable and Sustainable Energy Reviews 2018;81:655–68. https://doi.org/10.1016/j.rser.2017.08.047.

[25] Kraa O, Ghodbane H, Saadi R, Ayad MY, Becherif M, Aboubou A, et al. Energy Management of Fuel Cell/ Supercapacitor Hybrid Source Based on Linear and Sliding Mode Control. Energy Procedia 2015;74:1258–64. https://doi.org/10.1016/j.egypro.2015.07.770.

[26] Song K, Li F, Hu X, He L, Niu W, Lu S, et al. Multi-mode energy management strategy for fuel cell electric vehicles based on driving pattern identification using learning vector quantization neural network algorithm. Journal of Power Sources 2018;389:230–9. https://doi.org/10.1016/j.jpowsour.2018.04.024.

[27] Ahmadi S, Bathaee SMT, Hosseinpour AH. Improving fuel economy and performance of a fuel-cell hybrid electric vehicle (fuel-cell, battery, and ultra-capacitor) using optimized energy management strategy. Energy Conversion and Management 2018;160:74–84. https://doi.org/10.1016/j.enconman.2018.01.020.

[28] Corrêa JM, Farret FA, Gomes JR, Simões MG. Simulation of fuel-cell stacks using a computer-controlled power rectifier with the purposes of actual high-power injection applications. IEEE Transactions on Industry Applications 2003;39:1136–42.

[29] Wipke KB, Cuddy MR, Burch SD. ADVISOR 2.1: A user-friendly advanced powertrain simulation using a combined backward/forward approach. IEEE Transactions on Vehicular Technology 1999;48:1751–61. https://doi.org/10.1109/25.806767.

[30] Han J, Charpentier J-F, Tang T. An energy management system of a fuel cell/battery hybrid boat. Energies 2014;7:2799–820.

[31] Liso V, Nielsen MP, Kær SK, Mortensen HH. Thermal modeling and temperature control of a PEM fuel cell system for forklift applications. International Journal of Hydrogen Energy 2014;39:8410–20. https://doi.org/10.1016/J.IJHYDENE.2014.03.175.

[32] Arat HT, Sürer MG, Gökpinar S, Aydin K. Conceptual design analysis for a lightweight aircraft with a fuel cell hybrid propulsion system. Energy Sources, Part A: Recovery, Utilization, and Environmental Effects 2020:1–15.

[33] Chavan SL, Talange DB. Statistical design of experiment approach for modeling and optimization of PEM fuel cell. Energy Sources, Part A: Recovery, Utilization, and Environmental Effects 2018;40:830–46.

[34] Huang L, Chen J, Liu Z. Adaptive thermal control for PEMFC systems with guaranteed performance. International Journal of Hydrogen Energy 2018;43:11550–8. https://doi.org/10.1016/J.IJHYDENE.2017.12.121.

[35] Becherif M, Claude F, Hervier T, Boulon L. Multi-stack Fuel Cells Powering a Vehicle. Energy Procedia 2015;74:308–19. https://doi.org/10.1016/J.EGYPRO.2015.07.613.

[36] Ramadan HSM, de Bortoli Q, Becherif M, Claude F. Multi-stack fuel cell efficiency enhancement based on thermal management. IET Electrical Systems in Transportation 2016;7:65–73.

[37] Ahmaditaba AH, Afshari E, Asghari S. An experimental study on the bubble humidification method of polymer electrolyte membrane fuel cells. Energy Sources, Part A: Recovery, Utilization, and Environmental Effects 2018;40:1508–19.

[38] Feng J, Han J, Hou T, Peng X. Performance analysis and parametric studies on the primary nozzle of ejectors in proton exchange membrane fuel cell systems. Energy Sources, Part A: Recovery, Utilization, and Environmental Effects 2020:1–20.

[39] Pachauri RK, Chauhan YK, Gupta A. Proton exchange membrane fuel cells: Investigation of control schemes for reactants' flow pressure. Energy Sources, Part A: Recovery, Utilization, and Environmental Effects 2017;39:75–82.

[40] Yang Y, Zhang X, Guo L, Liu H. Local degradation in proton exchange membrane fuel cells with dead-ended anode. Journal of Power Sources 2020;477:229021.

[41] Pessot A, Turpin C, Jaafar A, Soyez E, Rallières O, Gager G, et al. Contribution to the modelling of a low temperature PEM fuel cell in aeronautical conditions by design of experiments. Mathematics and Computers in Simulation 2019;158:179–98.

[42] El Aabid S, Régnier J, Turpin C, Rallières O, Soyez E, Chadourne N, et al. A global approach for a consistent identification of static and dynamic phenomena in a PEM Fuel Cell. Mathematics and Computers in Simulation 2019;158:432–52.

[43] Amphlett JC, Baumert RM, Mann RF, Peppley BA, Roberge PR, Harris TJ. Performance modeling of the Ballard Mark IV solid polymer electrolyte fuel cell: I. Mechanistic model development. Journal of the Electrochemical Society 1995;142:1.